Materials Research Proceedings 69 (2026) 408-413 https://doi.org/10.21741/9781644904251-74

Dynamic Modeling of Rotor Damper Configurations for Aeroelastic and Ground Resonance Analysis

Matteo CROCI[1,a] and Pierangelo MASARATI[1,b,*]

[1]Department of Aerospace Science and Technology, Politecnico di Milano, via La Masa 34, Milano, Italy

[a]matteo6.croci@mail.polimi.it, [b]pierangelo.masarati@polimi.it

Keywords: Interblade Damper, Helicopter Rotor, Ground Resonance

Abstract. This paper presents the formulation and sensitivity analysis of ground resonance stability in rotorcraft equipped with unconventional lead-lag damping configurations, including the inter-blade and the recently proposed inter-2-blade arrangements. The developed framework enables consistent linearization of the coupled rotor-airframe system and supports comparison of the stability performance of conventional and novel damper configurations.

Introduction

Ground Resonance (GR) is a dynamic instability typical of helicopters, caused by the adverse coupling between the cyclic lead-lag motion of the blades and the motion of the airframe acting as a flexible support. It arises when the frequency of the slow first-order cyclic lead-lag mode approaches that of either the longitudinal (pitch) or lateral (roll) airframe motion [1].

Helicopter rotors are commonly equipped with damping devices to prevent such instability. The most conventional configuration employs dampers directly connecting each blade to the hub (BTH). Alternative arrangements connect the blades in different ways, often bypassing the hub. Among these, the “inter-blade” (IB) configuration couples adjacent blades, while the “inter-2-blade” (I2B) configuration connects non-adjacent blades [2, 3]. These concepts offer potential advantages partly explored in earlier studies.

The objectives of this work are:

- to develop a framework describing the exact kinematics of damper activation as a function of blade motion,
- to couple the consistently linearized damper-blade kinematics with industry-grade rotorcraft aeroelastic solvers,
- to formulate a consistent sensitivity analysis of the GR eigensolution,
- to assess the stability performance of the three configurations (BTH, IB, I2B), including selected damper-failure conditions.

The GR problem is analyzed by linearizing about steady reference equilibrium conditions.
The kinematics are derived by consistently linearizing a geometrically exact multibody model. For the nominal isotropic rotor, the system obtained through the multiblade coordinate transformation is linear and time-invariant and is treated using standard eigenanalysis.

Blade Lag Dynamics. Following Coleman's formulation [1], the linearized lead-lag dynamics of the *m*th blade in a rotor with three or more blades is expressed as

$$I_\xi \ddot{\xi}^{(m)} + \left(e S_\xi \Omega^2 + k_\xi\right) \xi^{(m)} = \tau_{\text{damper}}^{(m)} - S_\xi \ddot{y} \cos\psi_m + S_\xi \ddot{x} \sin\psi_m \tag{1}$$

with $m = 1..N_b$, and the damping torques are

$$\tau_{\text{damper}}^{(m)} = -c_\xi \begin{cases} \dot{\xi}^{(m)} & \text{BTH} \\ 2\dot{\xi}^{(m)} - \dot{\xi}^{(m-1)} - \dot{\xi}^{(m+1)} & \text{IB} \\ 2\dot{\xi}^{(m)} - \dot{\xi}^{(m-2)} - \dot{\xi}^{(m+2)} & \text{I2B} \end{cases} \tag{2}$$

Equation (1) is azimuth-dependent because the forcing terms associated with the airframe roll and pitch through the corresponding lateral and longitudinal accelerations depend on the blade azimuth $\psi_m = \psi + 2\pi\, m/N\_b$.

Multiblade Coordinates. For identical, equally spaced blades (isotropic rotor), introducing the multiblade (Coleman) transformation eliminates azimuth dependence:

$$\xi^{(m)} = \xi_0 + \sum_{n=1}^{\text{fix}((N_b-1)/2)} \left[\cos(n\psi_m)\xi_{nc} + \sin(n\psi_m)\xi_{ns}\right] + (-1)^m \xi_{N_b/2} \tag{3}$$

The last term applies only to even N_b. The transformation can be written compactly as

$$\boldsymbol{\xi}_b = \mathbf{T}(\psi)\boldsymbol{\xi} \qquad \dot{\boldsymbol{\xi}}_b = \dot{\mathbf{T}}(\psi)\boldsymbol{\xi} + \mathbf{T}(\psi)\dot{\boldsymbol{\xi}} \qquad \ddot{\boldsymbol{\xi}}_b = \ddot{\mathbf{T}}(\psi)\boldsymbol{\xi} + 2\dot{\mathbf{T}}(\psi)\dot{\boldsymbol{\xi}} + \mathbf{T}(\psi)\ddot{\boldsymbol{\xi}} \tag{4}$$

Here, $\boldsymbol{\xi}$ denotes the multiblade coordinates, $\boldsymbol{\xi}_b$ the individual blade coordinates, and $\mathbf{T}(\psi)$ the azimuth-dependent transformation matrix.

Coupled Rotor-Airframe Equations. After algebraic manipulation, the coupled rotor-airframe equations can be expressed as

$$\begin{aligned} &\begin{bmatrix} N_b I_\xi/2 & 0 & 0 & N_b S_\xi/2 \\ 0 & N_b I_\xi/2 & -N_b S_\xi/2 & 0 \\ 0 & -N_b S_\xi/2 & M_x + N_b M_b & 0 \\ N_b S_\xi/2 & 0 & 0 & M_y + N_b M_b \end{bmatrix} \begin{Bmatrix} \ddot{\xi}_{1c} \\ \ddot{\xi}_{1s} \\ \ddot{x} \\ \ddot{y} \end{Bmatrix} \\ &+ \begin{bmatrix} N_b \Xi_\clubsuit c_\xi/2 & N_b I_\xi \Omega & 0 & 0 \\ -N_b I_\xi \Omega & N_b \Xi_\clubsuit c_\xi/2 & 0 & 0 \\ 0 & 0 & C_x & 0 \\ 0 & 0 & 0 & C_y \end{bmatrix} \begin{Bmatrix} \dot{\xi}_{1c} \\ \dot{\xi}_{1s} \\ \dot{x} \\ \dot{y} \end{Bmatrix} \\ &+ \begin{bmatrix} N_b\left[\Xi_\clubsuit k_\xi + (eS_\xi - I_\xi)\Omega^2\right]/2 & N_b \Xi_\clubsuit c_\xi \Omega/2 & 0 & 0 \\ -N_b \Xi_\clubsuit c_\xi \Omega/2 & N_b\left[\Xi_\clubsuit k_\xi + (eS_\xi - I_\xi)\Omega^2\right]/2 & 0 & 0 \\ 0 & 0 & K_x & 0 \\ 0 & 0 & 0 & K_y \end{bmatrix} \begin{Bmatrix} \xi_{1c} \\ \xi_{1s} \\ x \\ y \end{Bmatrix} = \begin{Bmatrix} 0 \\ 0 \\ 0 \\ 0 \end{Bmatrix} \end{aligned} \tag{5}$$

with $\Xi_{\text{BTH}} = 1$, $\Xi_{\text{IB}} = 2(1 - \cos(2\pi/N_b))$, and $\Xi_{\text{I2B}} = 2(1 - \cos(4\pi/N_b))$, the latter two for ideal damping, i.e., directly proportional to the respective combinations of blade rotation.

The remaining multiblade coordinates remain decoupled from the airframe and are not discussed here. In the IB and I2B configurations, the collective motion receives no damping, and higher-order cyclic or reactionless I2B equations experience reduced damping compared with IB and BTH [3].

Damper Activation Kinematics. In practical designs, the damper activation depends on the relative motion of the blades through nonlinear kinematic relationships. Let $\varphi^{(m)}$ denote the activation of the mth damper (relative rotation or displacement),

$$\boldsymbol{\phi}^{(m)}\left(\mathbf{x}^{(m)}, \boldsymbol{\xi}_b\right) = \mathbf{0} \tag{6}$$

that represents the scleronomic constraint equations, where $\mathbf{x}^{(m)}$ collects the internal coordinates of the damper, with $\varphi^{(m)} = \varphi^{(m)}(\mathbf{x}^{(m)})$ (without excessive loss of generality, $\varphi^{(m)}$ can directly be an element of $\mathbf{x}^{(m)}$, or a linear combination, $\varphi^{(m)} = \mathbf{C}\,\mathbf{x}^{(m)}$; in the following, the superscript (m) will be

Materials Research Proceedings 69 (2026) 408-413 https://doi.org/10.21741/9781644904251-74

omitted for ease of notation). $\boldsymbol{\phi}$ contains as many equations as internal coordinates $\mathbf{x}$. The blade rotations, $\boldsymbol{\xi}_b$, are the independent variables. Equation (6) is solved to determine $\mathbf{x}$ as a function of $\boldsymbol{\xi}_b$, and thus determine the reference configuration of the damper system for a given reference blade lag rotation.

Linearization of Eq. (6) around the reference configuration yields

$$\Delta\mathbf{x} = -\boldsymbol{\phi}_{/\mathbf{x}}^{-1}\boldsymbol{\phi}_{/\boldsymbol{\xi}_b}\Delta\boldsymbol{\xi}_b \qquad \text{and} \qquad \Delta\varphi = -\mathbf{C}\boldsymbol{\phi}_{/\mathbf{x}}^{-1}\boldsymbol{\phi}_{/\boldsymbol{\xi}_b}\Delta\boldsymbol{\xi}_b = \boldsymbol{\Psi}\Delta\boldsymbol{\xi}_b \tag{7}$$

where submatrix $\boldsymbol{\phi}_{/\mathbf{x}}$ of the constraint Jacobian matrix is square by assumption and invertible as long as the closed kinematic chain it describes is not in a singular configuration. In the ideal BTH case, $\boldsymbol{\Psi}_i^{(m)} = \delta_{im}$, where δ_{im} is Kronecker's operator; in the ideal IB case, $\boldsymbol{\Psi}_i^{(m)} = \delta_{im}$ and $\boldsymbol{\Psi}_{i+1}^{(m)} = -\delta_{im}$; finally, in the ideal I2B case, $\boldsymbol{\Psi}_{i-1}^{(m)} = \delta_{im}$ and $\boldsymbol{\Psi}_{i+1}^{(m)} = -\delta_{im}$.

Damper Contribution to Virtual Work. The virtual work of the mth damper is

$$\delta\mathcal{W}_{\text{damper}}^{(m)} = -\delta\varphi\left(c_\varphi\Delta\dot{\varphi} + k_\varphi\Delta\varphi\right) = -\delta\boldsymbol{\xi}_b^{\mathsf{T}}\boldsymbol{\Psi}^{\mathsf{T}}\left(c_\varphi\boldsymbol{\Psi}\Delta\dot{\boldsymbol{\xi}}_b + k_\varphi\boldsymbol{\Psi}\Delta\boldsymbol{\xi}_b\right) \tag{8}$$

where c_φ and k_φ are the linearized viscous and elastic characteristics of an elastomeric damper. In the ideal case, $c_\xi \equiv c_\varphi$ and $k_\xi \equiv k_\varphi$, whereas in practical cases, the kinematics of the lag activation mechanism hidden in $\boldsymbol{\Psi}$ need to be used.

Using the same reference configuration for all blades (e.g., the same reference lead-lag angle), the kinematic problem is solved for just one damper, and the same expression of Eq. (8) for the virtual work is used for all, simply changing the indexes of the involved blade rotations in $\boldsymbol{\xi}_b$. Stacking all dampers yields

$$\delta\mathcal{W}_{\text{dampers}} = \sum_m \delta\mathcal{W}_{\text{damper}}^{(m)} = -\delta\boldsymbol{\xi}_b^{\mathsf{T}}\mathbf{B}^{\mathsf{T}}\left(c_\varphi\mathbf{B}\Delta\dot{\boldsymbol{\xi}}_b + k_\varphi\mathbf{B}\Delta\boldsymbol{\xi}_b\right) \tag{9}$$

where

$$\mathbf{B}^{\mathsf{T}} = \left[\boldsymbol{\Psi}^{(1)^{\mathsf{T}}}, \ldots, \boldsymbol{\Psi}^{(N_b)^{\mathsf{T}}}\right]$$

A kinematically and energetically consistent definition of damper activation does not alter the structure of Eq. (5), only affecting the coefficients $\Xi_\clubsuit$. It also affects the remaining rotor equations, which, however, remain decoupled from the airframe motion.

Sensitivity of Eigensolution. Equation (5) can be written as

$$\left(s^2\mathbf{M}_c + s\mathbf{C}_c + \mathbf{K}_c\right)\mathbf{z} = \mathbf{0} \tag{10}$$

where $\mathbf{z}$ is the eigenvector and s the eigenvalue.

The sensitivity of the ℓth eigenpair to a generic parameter p is obtained by differentiating Eq. (10) and the L^∞ normalization condition $\mathbf{n}^{\mathsf{T}}\,\mathbf{z} = 1$ ($\mathbf{n} = [0, \ldots, 1, \ldots 0]^{\mathsf{T}}$) with respect to p, i.e.,

$$\begin{bmatrix} \left(s_\ell^2\mathbf{M}_c + s_\ell\mathbf{C}_c + \mathbf{K}_c\right) & \left(2s_\ell\mathbf{M}_c + \mathbf{C}_c\right)\mathbf{z}_\ell \\ \mathbf{n}^{\mathsf{T}} & \end{bmatrix} \begin{Bmatrix} \mathbf{z}_{\ell/p} \\ s_{\ell/p} \end{Bmatrix} = \begin{Bmatrix} -\left(s_\ell^2\mathbf{M}_{c/p} + s_\ell\mathbf{C}_{c/p} + \mathbf{K}_{c/p}\right)\mathbf{z}_\ell \\ 0 \end{Bmatrix} \tag{11}$$

If the damper kinematics depend on p, the corresponding derivatives include

$$\Delta\varphi_{/p} = -\mathbf{C}\boldsymbol{\phi}_{/\mathbf{x}}^{-1}\left(\boldsymbol{\phi}_{/\boldsymbol{\xi}_b p} - \boldsymbol{\phi}_{/\mathbf{x}p}\boldsymbol{\phi}_{/\mathbf{x}}^{-1}\boldsymbol{\phi}_{/\boldsymbol{\xi}_b}\right)\Delta\boldsymbol{\xi}_b = \boldsymbol{\Psi}_{/p}\Delta\boldsymbol{\xi}_b \tag{12}$$

while for parameters directly affecting system matrices, the computation is straightforward.

Damper Failure. If one or more dampers fail, the problem becomes time-periodic. Its stability can be studied using the Floquet-Lyapunov method [4], and its sensitivity can be derived following the procedure in [5].

Results

Realistic IB and I2B layouts, adapted from existing designs, are shown in Fig. 1. In the IB configuration (left), a rotational damper is attached to blade m and linked to blade $m + 1$ through a rigid connection. The model is treated as two-dimensional for clarity, but has also been implemented in 3D. Each sub-assembly consists of a blade, a damper, and a connecting link between the damper and the preceding blade, for a total of three bodies and nine DoF, eight of which are eliminated by the four hinges, leaving one DoF, the blade rotation. Each closed loop consists of four bodies and 12 DoF, 10 of which are eliminated by the five hinges, corresponding to a five-bar mechanism. Prescribing the rotations of the blades makes the problem kinematically determined. Using data from [6], the transmission ratio is $\mathbf{\Psi}(m, m + 1) = [-1.5045, 0.6320]$, which differs notably from the ideal $[-1, 1]$.

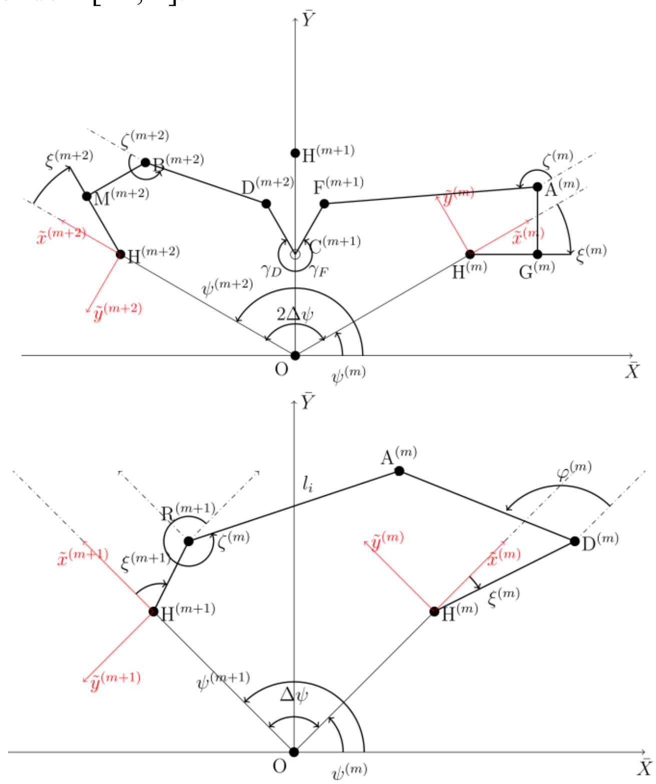

Figure 1: Realistic configurations: inter-blade (left) and inter-2-blade (right).

Figure 2 presents the coupled rotor-airframe eigensolution for the IB configuration. The top-left panel shows the real parts of all eigenvalues; the top-right highlights the critical mode (real and imaginary parts), the slow cyclic eigenvalue, which becomes unstable slightly above $\Omega_{100\%}$. The bottom panels show its sensitivity to the stiffnesses (left) and dampings (right) of the damper and the link's elastomeric bearings.

Using sensitivity analysis, equivalent BTH and I2B models were tuned by continuation. The equivalent BTH configuration was matched by adjusting k_ξ and c_ξ to reproduce the same slow cyclic eigenvalue as the IB case at $\Omega_{100\%}$. The equivalent I2B model was tuned by adjusting also other kinematic parameters to match the slow cyclic and also the collective eigenvalue, which is undamped in the ideal IB and I2B cases.

Figure 3 compares the real parts of the eigenvalues for the IB (left), I2B tuned for slow cyclic (center), and I2B tuned for both slow cyclic and collective modes (right) at $\Omega_{100\%}$. The results demonstrate strong similarity and comparable GR stability among the configurations.

Finally, results obtained with a detailed rotor and airframe aeroelastic model implemented in MASST [7], a general-purpose rotorcraft aeroelasticity tool, confirm the observed trends.

Materials Research Proceedings 69 (2026) 408-413 https://doi.org/10.21741/9781644904251-74

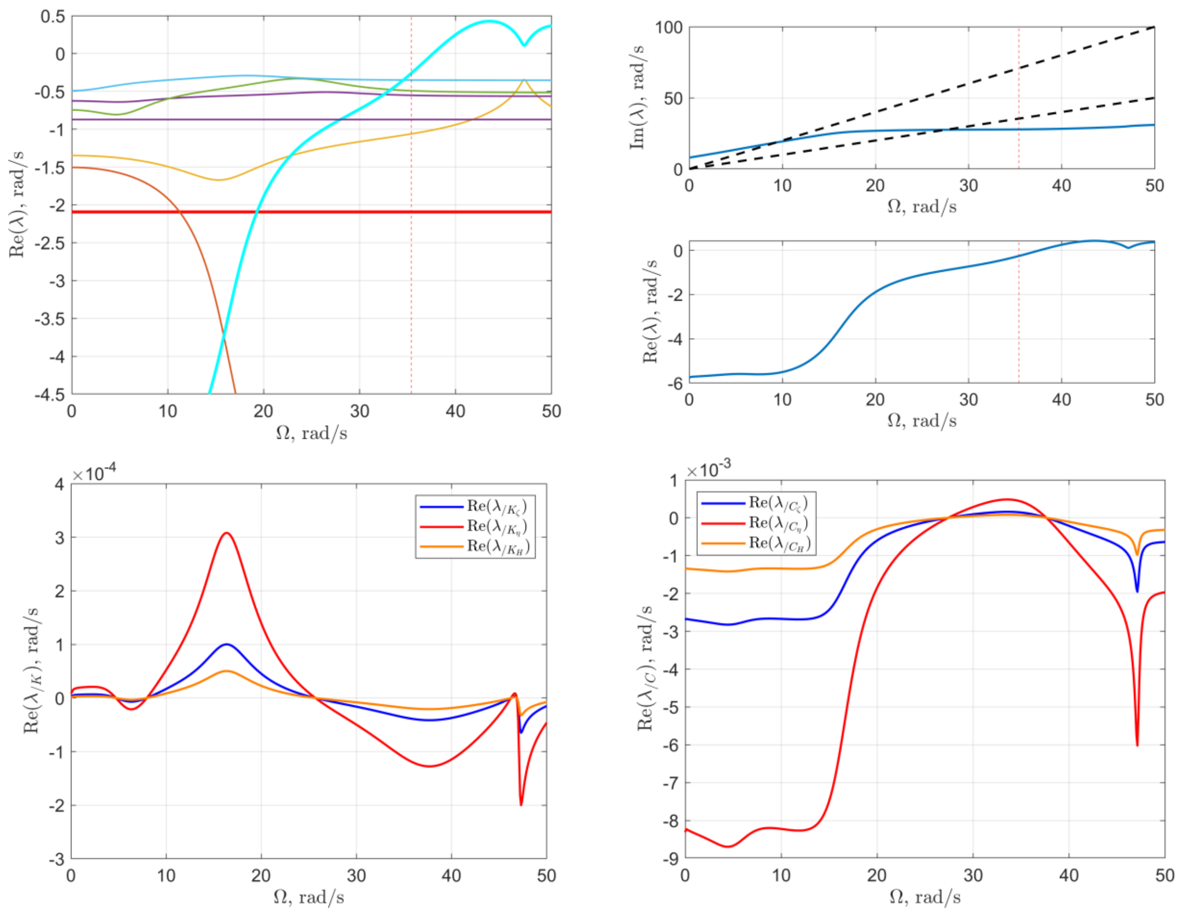

Figure 2: Realistic IB configuration: Re(s) ↖, critical Re(s) and Im(s) ↗, Re($s_{/k}$) ↙, Re($s_{/c}$) ↘.

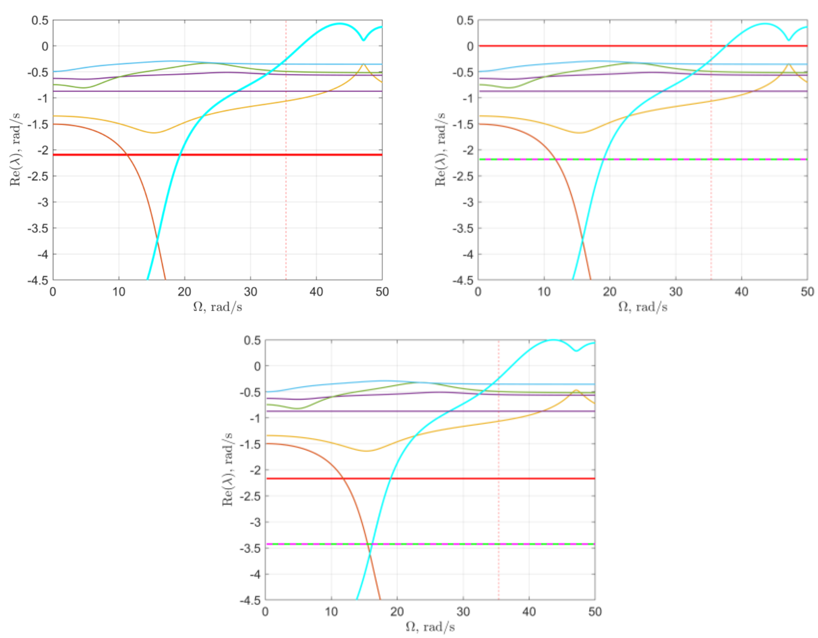

Figure 3: Comparison of configurations: IB (left), I2B tuned for slow cyclic (center), and for slow cyclic and collective (right).

Materials Research Proceedings 69 (2026) 408-413 https://doi.org/10.21741/9781644904251-74

References

[1] Robert P. Coleman. Theory of self-excited mechanical oscillations of hinged rotor blades. ARR 3G29, NACA, July 1943.

[2] Pierangelo Masarati and Leonardo Frison. Rotore per elicottero a smorzamento migliorato, 2021. Italian Patent No. 102021000018017

[3] Leonardo Frison, Andrea Zanoni, and Pierangelo Masarati. The inter-2-blade lead-lag damper concept. In 78th Forum of the Vertical Flight Society, Fort Worth, TX, USA, May 20–22, 2022. https://doi.org/10.4050/F-0078-2022-17524

[4] C. Eugene Hammond. An application of Floquet theory to prediction of mechanical instability. Journal of the American Helicopter Society, 19(4):14–23, 1974. https://doi.org/10.4050/JAHS.19.14

[5] Aykut Tamer and Pierangelo Masarati. Periodic stability and sensitivity analysis of rotating machinery. In Proceedings of the 9th International Conference on Rotor Dynamics IFToMM ICORD 2014, Milan, Italy, Sept. 22–25, 2014. https://doi.org/10.1007/978-3-319-06590-8_170

[6] Matteo Croci. Ground resonance sensitivity study for unconventional damper configurations. Master's thesis, Politecnico di Milano, 2025.

[7] Pierangelo Masarati, Vincenzo Muscarello, and Giuseppe Quaranta. Linearized aeroservoelastic analysis of rotary-wing aircraft. In 36th European Rotorcraft Forum, pages 099.1–10, Paris, France, September 7–9, 2010.